

## Validity range of canonical approach to finite density QCD

---

**Ryutaro Fukuda\***

*Institute für Theoretische Physik, ETH Zürich, CH-8093 Zürich, Switzerland*

*Department of Physics, The University of Tokyo, Tokyo 113-0033, Japan*

*E-mail: jr-fukuda@nt.phys.s.u-tokyo.ac.jp*

**Atsushi Nakamura**

*Research Center for Nuclear Physics, Osaka University, Ibaraki 567-0047, Japan*

*Theoretical Research Division, Nishina Center, RIKEN, Wako 351-0198, Japan*

*School of Biomedicine, Far Eastern Federal University, Vladivostok, 690950, Russia*

**Shotaro Oka**

*Department of Physics, Rikkyo University, Tokyo 171-8501, Japan*

In this study, we calculate pressure, baryon number density and baryon susceptibility at finite density through lattice QCD with the canonical approach which is a fugacity expansion of grand canonical partition function. We compare the results with those obtained using the multi-parameter reweighting (MPR) method. The results of these methods were found to be in very good agreement in the regions where the errors of the MPR method are under control. Moreover, our canonical approach works beyond  $\mu_B/T = 3$  in many cases.

*The 33rd International Symposium on Lattice Field Theory*

*14 -18 July 2015*

*Kobe International Conference Center, Kobe, Japan\**

---

\*Speaker.

## 1. Introduction

Although it is well known that QCD has a rich phase structure on a temperature-density plane[1], the investigations with a first-principles calculation are limited in a small density region due to the so-called sign problem[2]. However, in finite temperature and density QCD systems, a lot of physically interesting targets such as the early universe, neutron stars and quark matters have been waiting to be explored. Therefore, it can be said that it is quite meaningful to seek methods for accurate computation of thermodynamic quantities at large chemical potential values: this is an urgent subject in the fields of particle and nuclear physics.

The canonical approach[3, 4, 5, 6] which is studied in this work probably has a potential to overcome the sign problem. This is because it can avoid the sign problem in an artful manner. However, it is reported that it has its particular numerical instabilities[7] and it is somewhat unclear whether it can produce reliable results. Taking this situation into consideration, in this work, we discuss the validity range of the canonical approach comparing directly with the results obtained by the MPR method[8].

## 2. Frame work

### 2.1 Canonical approach for finite density systems: fugacity expansion of grand canonical partition function

A system which obeys the grand canonical ensemble is consistent with a system which obeys the canonical ensemble in thermodynamic limit. Standing on this fundamental idea, the canonical approach can be interpreted as a polynomial expansion method of a grand canonical partition function  $Z_{GC}(T, \mu_B)$  at temperature  $T$  and baryon chemical potential  $\mu_B$  in terms of canonical partition functions  $Z_C(B, T)$  and fugacity  $\exp(\mu_B/T)$  as follows:

$$Z_{GC}(T, \mu_B) = \sum_{B=-\infty}^{\infty} Z_C(B, T) e^{B\mu_B/T}, \quad (2.1)$$

where  $B$  is not net quark number but net baryon number[3, 4, 9]. If the canonical partition functions at all fixed net baryon number sectors can be obtained once, one can calculate expectation values of thermodynamic observables at any real baryon chemical potential values. This is because the baryon chemical potential dependence of the grand canonical partition function in a context of the canonical approach can be tuned only by fugacity. This feature is a major advantage of canonical approach in view of the numerical computation. The largest advantage of the canonical approach is to be able to avoid the sign problem. To be more specific, canonical partition functions can be calculated through Fourier transformation of the grand canonical partition function computed at pure imaginary chemical potential values:

$$Z_C(B, T) = \frac{1}{2\pi} \int_0^{2\pi} d\left(\frac{\mu_I}{T}\right) Z_{GC}(T, i\mu_I) e^{iB\mu_I/T}, \quad (2.2)$$

where  $\mu_I \in \mathbb{R}$ . Therefore, in the canonical approach, it is essential to calculate grand canonical partition functions at various pure imaginary chemical potential values to perform the Fourier transformation for calculating canonical partition functions.

## 2.2 Winding number expansion method

In this work, the following simplest reweighting method for a fermion determinant is adopted in the calculation of grand canonical partition functions at pure imaginary chemical potential.

$$Z_{GC}(T, i\mu_I) = \int [dU] \left( \frac{\det \Delta(i\mu_I)}{\det \Delta(\mu_0)} \right) \det \Delta(\mu_0) e^{-S_g} \quad (2.3)$$

Here,  $\Delta(\mu)$  is a fermion matrix and  $S_g$  is a gauge action. The chemical potential  $\mu_0$  in Eq.(2.3) can be set to zero or any pure imaginary values. Considering to perform a Monte Carlo integration with a weight  $\det \Delta(\mu_0) e^{-S_g}$  in Eq.(2.3), the expectation value of the grand canonical partition functions at pure imaginary chemical potential normalized by a grand canonical partition function at the chemical potential  $\mu_0$  can be given by the following way.

$$\begin{aligned} \left\langle \frac{Z_{GC}(T, i\mu_I)}{Z_{GC}(T, \mu_0)} \right\rangle_{\mu_0} &= \frac{1}{Z_{GC}(T, \mu_0)} \int [dU] \left( \frac{\det \Delta(T, i\mu_I)}{\det \Delta(T, \mu_0)} \right) \det \Delta(T, \mu_0) e^{-S_g} \\ &= \left\langle \frac{\det \Delta(T, i\mu_I)}{\det \Delta(T, \mu_0)} \right\rangle_{\mu_0} \end{aligned} \quad (2.4)$$

Using this relation, Eq.(2.2) can be rewritten as

$$\frac{Z_C(B, T)}{Z_{GC}(T, \mu_0)} = \frac{1}{2\pi} \int_0^{2\pi} d\left(\frac{\mu_I}{T}\right) \left\langle \frac{\det \Delta(T, i\mu_I)}{\det \Delta(T, \mu_0)} \right\rangle_{\mu_0} e^{iB\mu_I/T}. \quad (2.5)$$

The extra constant  $1/Z_{GC}(T, \mu_0)$  in the left-hand side of Eq.(2.5) is irrelevant in actual numerical calculations. This is because for example one can avoid the constant to define normalized canonical partition functions as  $Z_C(B, T)/Z_C(B=0, T)$ .

In this work, we adopt the Wilson fermion formalism and we use a winding number expansion based on the hopping parameter expansion to calculate expectation values of the fermion determinant assuming that quarks are heavy enough. In general, Wilson fermion matrix  $\Delta(T, \mu)$  can be written as

$$\Delta(T, \mu) = 1 - \kappa Q_s - \kappa Q_t(T, \mu) \equiv 1 - \kappa Q(T, \mu), \quad (2.6)$$

where  $\kappa$  is the hopping parameter,  $Q_s$  and  $Q_t$  correspond to the hopping term in the three dimensional space direction and in the time direction, respectively. Therefore, a logarithm of the fermion determinant can be written as

$$\log \det \Delta(T, i\mu_I) = \text{Tr} \log \Delta(T, i\mu_I) = - \sum_{n=1}^{\infty} \frac{\kappa^n}{n} \text{Tr} Q^n(T, i\mu_I) \quad (2.7)$$

The trace in Eq.(2.7) is taken over spacetime, spinor and color indices. Taking into account the feature of the hopping term  $Q$  in the trace in Eq.(2.7), one can easily find that all non-zero contribution of the trace comes from any closed loops on a lattice. Moreover, it can be said that the chemical potential dependence comes only from any closed loops which are winding along positive or negative time directions through the anti-periodic boundary condition considering the introduction of the quark chemical potential onto the link variables in the time direction. For example, a trace of a closed loop which is winding along positive time direction  $n$  times can be evaluated as

$Ce^{im\mu_0/T}$ , where  $C$  is complex constant. Thus, if one classifies all closed loops in Eq.(2.7) according to “winding number” which is the number of net windings along the time direction, as a result, one can analytically reach the following expression with complex coefficients  $W_n$  and the complex fugacity  $e^{i\mu_l/T}$

$$\det\Delta(i\mu_l) = \exp \left[ \sum_{n=-\infty}^{\infty} W_n e^{in\mu_l/T} \right], \quad (2.8)$$

where  $n$  represents the winding number. In practical numerical calculations, one can approximately evaluate the complex coefficients  $W_n$  up to  $\pm N$  th order performing the hopping parameter expansion up to  $N_t \times N$  th order, where  $N_t$  is the size of a lattice in the time direction. A major advantage of this method is to be able to significantly reduce numerical costs for the calculation of the fermion determinant because if one calculates  $W_n$  with one gauge configuration generated at  $\mu_0$ , one can compute all fermion determinants at any pure imaginary chemical potential values for the gauge configuration. On the other hand, the numerical costs are rather expensive in case of using an exact calculation method for the fermion determinant. Therefore, in this instance, it is so hard to adopt a sufficiently large lattice size with recent computational resources. Moreover, the main aim of this work is to investigate if the canonical approach works well. Taking these circumstances into consideration, it can be suitable for this work to adopt a winding number expansion for realizing simple and meaningful numerical analyses as a kind of test.

### 3. Numerical results

#### 3.1 Lattice design and calculation procedure

We adopted a two-flavor clover-improved Wilson fermion action and Iwasaki gauge action. All simulations were performed on an  $8^3 \times 4$  lattice at temperatures of  $T/T_c = 1.35(7)$ ,  $1.20(6)$ ,  $1.08(5)$ ,  $0.99(5)$ ,  $0.93(5)$  and  $0.84(4)$  and  $m_\pi/m_\rho = 0.8$ , as in Ref.[10]. All gauge configurations at each temperature were generated at  $\mu_0 = 0$  using the hybrid Monte Carlo (HMC) method. Coefficients  $W_n$  in Eq.(2.8) were approximately computed up to  $\pm n = 120$  using the hopping parameter expansion up to  $120 \times N_t$  th order with 400 configurations in all temperature cases. We used 64 and 128 noise vectors for temperatures above and below  $T_c$ , respectively, to calculate the trace in Eq.(2.7). Canonical partition functions were evaluated through the Fourier transformation of the fermion determinant calculated by the winding number expansion. For this Fourier transformation, a multiple precision calculation with the numerical library FPLib[11] was adopted with 400 significant digits. This is because the Fourier transformation is an oscillatory integral and cancellation of significant digits are not negligible in the calculation. Multiple precision calculation plays an important role to reduce the numerical instability in the canonical approach. For the detailed discussion, see Ref.[12].

#### 3.2 Thermodynamic observables

In this work, we calculate the baryon chemical potential dependence of a dimensionless pressure  $\Delta p/T^4$ , baryon number density  $n_B/T^3$  and baryon susceptibility  $\chi_B/T^2$ :

$$\frac{\Delta p(\mu_B, T)}{T^4} = \frac{p(\mu_B, T)}{T^4} - \frac{p(0, T)}{T^4} = \left( \frac{N_t}{N_s} \right)^3 \log \left( \frac{Z_{GC}(\mu_B, T)}{Z_{GC}(0, T)} \right),$$

$$\frac{n_B(\mu_B, T)}{T^3} = \frac{\partial}{\partial(\mu_B/T)} \frac{p(\mu_B, T)}{T^4}, \quad \chi(\mu_B, T) = \frac{\partial^2}{\partial(\mu_B/T)^2} \frac{p(\mu_B, T)}{T^4}, \quad (3.1)$$

where  $N_s = N_x = N_y = N_z$  and  $T^{-1} = N_t a$  for a lattice spacing of  $a$ . In the following, we discuss the validity range of the canonical partition function comparing our canonical results with MPR results in Ref.[13].

### 3.2.1 Pressure

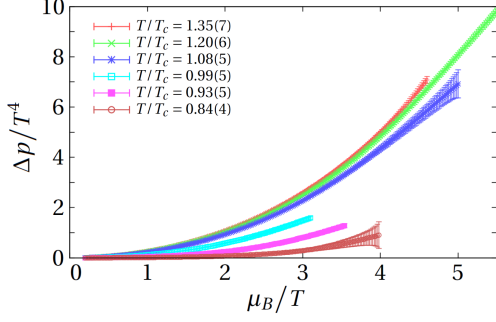


**Figure 1:** Baryon chemical potential dependence of pressure.

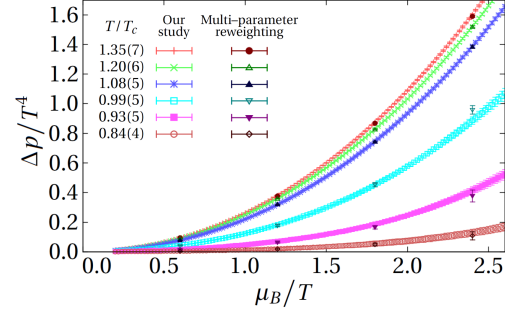


**Figure 2:** Comparison of pressure calculated by the canonical approach and the MPR method.

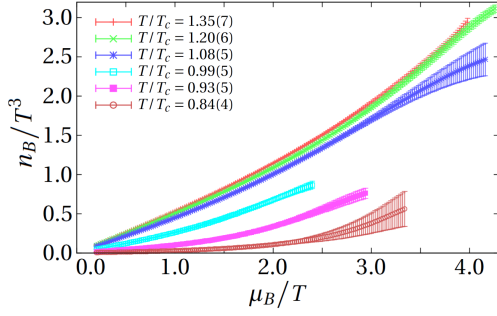
Fig.1 shows the baryon chemical potential dependence of pressure calculated by our canonical method. This shows that the pressure at above  $T_c$  are free enough from statistical errors up to  $\mu_B/T$  of approximately 5, and the results at below  $T_c$  are reliable up to  $\mu_B/T$  of approximately 3.5–4. On the other hand, the results at just below  $T_c$  are reliable only up to  $\mu_B/T$  of approximately 3. This is because we generated configurations at  $\mu_0 = 0$ . Namely, they suffered from fluctuations caused by the confined-deconfined phase transition located around zero density region.

Fig.2 is the comparison of pressure calculated by the canonical approach and MPR method. This shows that in low density region where statistical errors of MPR method are under our control, the canonical approach can produce completely consistent pressure results with those calculated by MPR method.

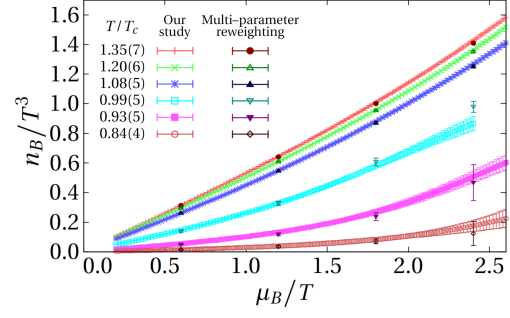
### 3.2.2 Baryon number density

Fig.3 shows the baryon chemical potential dependence of baryon number density computed by our canonical method. This demonstrates that for above and below  $T_c$  case, the results are reliable up to  $\mu_B/T$  of approximately 4 and 3–3.5, respectively, whereas the reliable baryon chemical potential range of the results for just below  $T_c$  case are limited for  $\mu_B/T$  of up to 2.4. This may be for the same reason described in the pressure analysis. Moreover, as a whole the reliable baryon chemical range is limited more than that of pressure. This can be interpreted that the convergence of the fugacity expansion for baryon number density becomes worse due to the first-order differentiation in terms of  $\mu_B/T$  as shown in Eq.(3.1).

Fig.4 is the comparison of baryon number density calculated by the canonical approach and the MPR method. This shows good agreement between the results of the canonical approach and those of the MPR method also in the baryon number density case. Paying attention to the temperature dependence of the baryon number density, the gradient as a function of the baryon chemical



**Figure 3:** Baryon chemical potential dependence of baryon number density.



**Figure 4:** Comparison of the baryon number densities calculated by the canonical approach and the MPR method.

potential becomes smaller as the temperature decreases. In the zero temperature case,  $n_B$  is phenomenologically expected to be zero up to  $\mu_B/T = m_B/T$ , where  $m_B$  is the lightest baryon mass of the system, and becomes a finite value at this point. For example, the data at  $T/T_c = 0.84$  in Fig.3 indicates such a feature in fact.

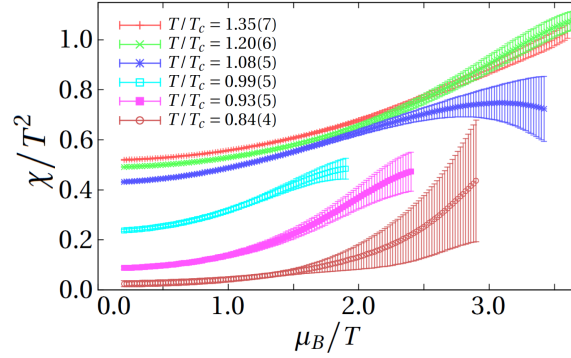


**Figure 5:** Chemical potential dependence of baryon susceptibility.

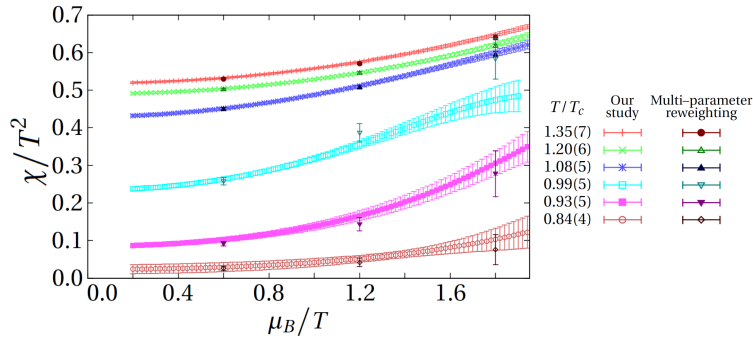


**Figure 6:** Comparison of baryon susceptibilities calculated by the canonical approach and the MPR method.

### 3.2.3 Baryon susceptibility

Fig.5 demonstrates the baryon chemical potential dependence of baryon susceptibility com-

puted by our canonical method. This shows that the results at temperatures above  $T_c$  are reliable up to a ratio  $\mu_B/T$  of approximately 3.5, whereas those at temperatures below  $T_c$  are reliable up to  $T_c = 2.4 - 2.9$ . The baryon susceptibility as a function of  $\mu_B/T$  does not show a clear peak, and thus the signal of the transition between the confined and deconfined phases at finite density cannot yet be observed.

Fig.6 is the comparison of baryon susceptibility calculated by the canonical approach and MPR method. From Fig.6, we find that the susceptibility results of the canonical approach are in very good agreement with those of the MPR method.

#### 4. Summary

In this work, we checked the canonical approach could produce consistent results with those calculated by the MPR method in the low density region. Moreover, the canonical approach provided reliable results beyond  $\mu_B/T = 3$  for almost all observables. Although we need to calculate canonical partition functions more accurately at large baryon numbers to get more reliable signals of thermodynamic quantities at large baryon chemical potential regions, our results are very encouraging for the first-principles calculation of finite density QCD.

#### Acknowledgments

This study was conducted for Zn Collaboration. We would like to thank the members of Zn Collaboration, S. Sakai, A. Suzuki and Y. Taniguchi for their support. R. F. also appreciates the useful discussions with K. Fukushima and Ph. de Forcrand. The calculations were performed with SX-9 and SX-ACE at the Research Center for Nuclear Physics (Osaka) and SR16000 at the Yukawa Institute for Theoretical Physics (Kyoto).

#### References

- [1] K. Fukushima and T. Hatsuda, Rept. Prog. Phys. **74**, 014001 (2011).
- [2] Ph. de Forcrand, PoS (LAT2009), 010 (2009).
- [3] A. Hasenfratz and D. Toussaint, Nucl. Phys B371 (1992), 539.
- [4] P. de Forcrand and S. Kratochvila, Nucl. Phys. Proc. Suppl. **153**, 62 (2006) [hep-lat/0602024].
- [5] C. Gattringer, H. -P. Schadler, Phys. Rev. D **91**, 074511 (2015) [arXiv:1411.5133 [hep-lat]].
- [6] A. Nakamura, S. Oka and Y. Taniguchi, arXiv:1504.04471.
- [7] X. Meng *et al.*, PoS (LAT2008), 032 (2008) [arXiv:0811.2112].
- [8] Z. Fodor, S. D. Katz, JHEP, 014 (2002). (hep-lat/0106002)
- [9] A. Roberge and N. Weiss, Nucl. Phys. B275(1986) 734.
- [10] WHOT-QCD Collaboration, S. Ejiri *et al.*, Phys. Rev. D **82**, 014508 (2010).
- [11] D. M. Smith, <http://myweb.lmu.edu/dmsmith/FMLIB.html>
- [12] R. Fukuda, A. Nakamura and S. Oka, arXiv:1504.06351.
- [13] K. Nagata and A. Nakamura, JHEP, 1204, 092 (2012) [arXiv:1201.2765].